Polymer Journal, Vol. 2, No. 1, pp 62-73 (1971)

Normal-Coordinate Analysis of Poly(Vinyl Chloride) and Deuterated Analogs

Mitsuo TASUMI and Takehiko SHIMANOUCHI

Department of Chemistry, Faculty of Science, University of Tokyo, Bunkyo-ku, Tokyo, Japan.

(Received September 2, 1970)

ABSTRACT: Normal-vibration frequencies of the extended syndiotatic structure of poly(vinyl chloride) and deuterated analogs (α-d_1, β-d_1, α,β-d_2, β,β-d_2, and d_3) were calculated with the modified Urey—Bradley force field. The results were utilized to analyze the infrared spectra of these polymers and detailed assignments were given to most of the crystalline bands.

KEY WORDS Infrared Spectrum / Poly(Vinyl Chloride) / Deuterated Analogs / Normal Coordinate / Vibration Frequency / Force Field / Assignment/

It is well known that the analysis of the infrared and Raman spectra provide valuable information on the conformation, structural irregularity, crystallinity etc., of various high polymers. The first step of the spectral analysis is always the establishment of the band assignments for regular structures.

Previously we reported a normal-coordinate treatment and assignments of infrared-absorption bands of poly(vinyl chloride) (PVC) and fully deuterated species (PVC-d_3)[1]. However, the force field used at that time was rather crude, and it was desired to refine the force field, so that more definite assignments of bands could be obtained. Since then, we have studied the molecular vibrations of polyethylene and obtained a reliable set of force constants related to the CH_2 group[2]. In order to get the force constants of the CHCl group, we have calculated the normal frequencies of some small molecules containing the Cl atom such as CH_3CH_2Cl, $CH_3CHClCH_3$, and $(CH_3)_3CCl$.

Experimentally also, there have been several efforts to make the band assignments clearer. Inversion of dichroism was found for some bands with the degree of stretching the film. The interpretation of this fact furnished the basis for the assignments of bands to the symmetry species expected to the extended syndiotactic structure[3]. Highly syndiotactic (therefore highly crystalline) samples of PVC, PVC-α-d_1, PVC-β-d_1, PVC-α,β-d_2, and PVC-d_3 were prepared and their spectra were discussed by Krimm, *et al.*[4] Later PVC-β,β-d_2 was also studied by Enomoto, *et al.*[5]

The Raman spectra of normal and urea-complex PVC were studied by Koenig and Druesedow.[6] The results are in support of the infrared studies and are utilized in this paper also.

As we shall see below, the calculation by the use of a refined set of force constants provides systematic understanding of the bands of PVC and its deuterated analogs.

NORMAL-COORDINATE TREATMENT

Structure

In this study we are interested in the extended syndiotactic structure shown in Figure 1a. Here we assume that the bond angles around a carbon atom are tetrahedral and the bond lengths of CC, CH, and CCl bonds are, respectively, 1.54, 1.09, and 1.77Å. The structure has a glide plane (σ_g), a twofold axis (C_2), and a mirror plane (σ_v) which form the C_{2v} symmetry. This symmetry remains unaltered in PVC-α-d_1, PVC-β,β-d_2, and PVC-d_3, whereas PVC-β-d_1 and PVC-α,β-d_2 have lower symmetry because they lose the twofold axis passing through the methylene group. Furthermore, there can be various configurations associated with the β-deuterium (or hydrogen) atoms in these two polymers. In the present study we assume the disyndiotatic configurations

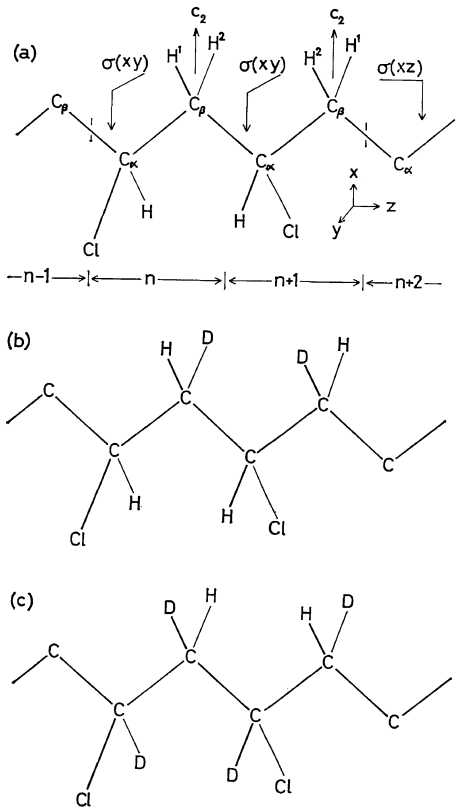

Figure 1. (a) Extended syndiotactic structure of PVC, (b) Disyndiotactic structure of PVC-β-d_1, and (c) Disyndiotactic structure of PVC-α,β-d_2.

Table I. Symmetry properties, number of normal modes, and selection rules of (a) PVC, PVC-α-d_1, PVC-β,β-d_2, and PVC-d_3 and (b) PVC-β-d_1 and PVC-α,β-d_2

	C_{2v}	E	C_2	σ_g	σ_v	n_i	IR	R
	A_1	1	1	1	1	9	M_x	a
(a)	A_2	1	1	−1	−1	7	f	a
	B_1	1	−1	1	−1	7	M_z	a
	B_2	1	−1	−1	1	9	M_y	a
	C_s	E		σ_g		n_i	IR	R
(b)	A'	1		1		16	M_x, M_z	a
	A''	1		−1		16	M_y	a

[a] n_i, number of normal modes; IR, infrared; R, Raman; a, active; f, forbidden.

illustrated in Figures 1b and 1c, which are the most probable structures expected for the polymers obtained by the γ-radiation polymerization of urea-complexes of pure monomers. The factor-group symmetry of the assumed disyndiotactic structure is C_s, since it has only a glide plane. Table I shows the symmetry analysis of the normal vibrations of the C_{2v} and C_s structures. The species A_1 and B_1 of the C_{2v} structure are correlated with the species A' of the C_s structure. Similarly A_2 and B_2 are correlated with A''. The transition moments of the A_1, B_2, and A'' vibrations are directed perpendicular to the chain, while those of B_1 are parallel and those of A' are either parallel or perpendicular.

Coordinates

The internal and local-symmetry coordinates are listed in Tables II and III, respectively.

Table II. Internal coordinates

$\Delta r_{\alpha n}^{Cl}$	$=C_{\alpha n}$—Cl stretching
$\Delta r_{\alpha n}^{H}$	$=C_{\alpha n}$—H stretching
$\Delta\Theta_{\alpha n}$	$=C_{\beta n-1}$—$C_{\alpha n}$—$C_{\beta n}$ bending
$\Delta\theta_{\alpha n}$	$=H_{\alpha n}$—$C_{\alpha n}$—Cl bending
$\Delta\gamma_{\alpha n}^{1}$	$=C_{\beta n-1}$—$C_{\alpha n}$—Cl bending
$\Delta\gamma_{\alpha n}^{2}$	$=C_{\beta n-1}$—$C_{\alpha n}$—H bending
$\Delta\gamma_{\alpha n}^{3}$	$=C_{\beta n}$—$C_{\alpha n}$—Cl bending
$\Delta\gamma_{\alpha n}^{4}$	$=C_{\beta n}$—$C_{\alpha n}$—H bending
$\Delta\gamma_n$	$=C_{\alpha n}$—$C_{\beta n}$ stretching
Δt_n	=Internal rotation[a] around $C_{\alpha n}$—$C_{\beta n}$
$\Delta r_{\beta n}^{1}$	$=C_{\beta n}$—H_n^1 stretching
$\Delta r_{\beta n}^{2}$	$=C_{\beta n}$—H_n^2 stretching
$\Delta\Theta_{\beta n}$	$=C_{\alpha n}$—$C_{\beta n}$—$C_{\alpha n+1}$ bending
$\Delta\theta_{\beta n}$	$=H_n^1$—$C_{\beta n}$—H_n^2 bending
$\Delta\gamma_{\beta n}^{1}$	$=C_{\alpha n}$—$C_{\beta n}$—H_n^1 bending
$\Delta\gamma_{\beta n}^{2}$	$=C_{\alpha n}$—$C_{\beta n}$—H_n^2 bending
$\Delta\gamma_{\beta n}^{3}$	$=C_{\alpha n+1}$—$C_{\beta n}$—H_n^1 bending
$\Delta\gamma_{\beta n}^{4}$	$=C_{\alpha n+1}$—$C_{\beta n}$—H_n^2 bending
$\Delta r_{n+1/2}$	$=C_{\beta n}$—$C_{\alpha n+1}$ stretching
$\Delta t_{n+1/2}$	=Internal rotation[a] around $C_{\beta n}$—$C_{\alpha n+1}$

[a] The definition of this coordinate is given in ref 2.

Some of the local-symmetry coordinates are different from what were used in the former study.[1] The coordinates related to the spectroscopically active vibrations (or factor-group vibrations) are given in Table IV.

Table III. Local-symmetry coordinates

$R^1_{\alpha n}=\Delta r^H_{\alpha n}$	CH stretching
$R^2_{\alpha n}=\Delta r^{Cl}_{\alpha n}$	CCl stretching
$R^3_{\alpha n}=\frac{1}{\sqrt{6}}(2\Delta\theta_{\alpha n}-\Delta\gamma^2_{\alpha n}-\Delta\gamma^4_{\alpha n})$	CH bending
$R^4_{\alpha n}=\frac{1}{\sqrt{6}}(\Delta\Theta_{\alpha n}-\Delta\theta_{\alpha n}+\Delta\gamma^1_{\alpha n}-\Delta\gamma^2_{\alpha n}+\Delta\gamma^3_{\alpha n}-\Delta\gamma^4_{\alpha n})$	Deformation 1
$R^5_{\alpha n}=\frac{1}{\sqrt{6}}(2\Delta\Theta_{\alpha n}-\Delta\gamma^1_{\alpha n}-\Delta\gamma^3_{\alpha n})$	Deformation 2
$R^6_{\alpha n}=\frac{1}{\sqrt{2}}(\Delta\gamma^2_{\alpha n}-\Delta\gamma^4_{\alpha n})$	CH wagging
$R^7_{\alpha n}=\frac{1}{\sqrt{2}}(\Delta\gamma^1_{\alpha n}-\Delta\gamma^3_{\alpha n})$	CCl wagging
$R^8_{\alpha n}=\Delta r_n$	CC stretching
$R^9_{\alpha n}=\Delta t_n$	Internal rotation
$R^1_{\beta n}=\frac{1}{\sqrt{2}}(\Delta r^1_{\beta n}+\Delta r^2_{\beta n})$	CH_2 symmetric stretching
$R^2_{\beta n}=\frac{1}{\sqrt{20}}(4\Delta\theta_{\beta n}-\Delta\gamma^1_{\beta n}-\Delta\gamma^2_{\beta n}-\Delta\gamma^3_{\beta n}-\Delta\gamma^4_{\beta n})$	CH_2 scissor
$R^3_{\beta n}=\frac{1}{\sqrt{30}}(5\Delta\Theta_{\beta n}-\Delta\theta_{\beta n}-\Delta\gamma^1_{\beta n}-\Delta\gamma^2_{\beta n}-\Delta\gamma^3_{\beta n}-\Delta\gamma^4_{\beta n})$	CCC bending
$R^4_{\beta n}=\frac{1}{2}(\Delta\gamma^1_{\beta n}-\Delta\gamma^2_{\beta n}-\Delta\gamma^3_{\beta n}+\Delta\gamma^4_{\beta n})$	CH_2 twisting
$R^5_{\beta n}=\frac{1}{\sqrt{2}}(\Delta r^1_{\beta n}-\Delta r^2_{\beta n})$	CH_2 antisymmetric stretching
$R^6_{\beta n}=\frac{1}{2}(\Delta\gamma^1_{\beta n}+\Delta\gamma^2_{\beta n}-\Delta\gamma^3_{\beta n}-\Delta\gamma^4_{\beta n})$	CH_2 wagging
$R^7_{\beta n}=\frac{1}{2}(\Delta\gamma^1_{\beta n}-\Delta\gamma^2_{\beta n}+\Delta\gamma^3_{\beta n}-\Delta\gamma^4_{\beta n})$	CH_2 rocking
$R^8_{\beta n}=\Delta r_{n+1/2}$	CC stretching
$R^9_{\beta n}=\Delta t_{n+1/2}$	Internal rotation

Table IV. Spectroscopically active coordinates

$A_1(A')$	$S_1=\frac{1}{\sqrt{2N}}\sum_n R^1_{\alpha n}$	CH stretching
	$S_2=\frac{1}{\sqrt{2N}}\sum_n R^2_{\alpha n}$	CCl stretching
	$S_3=\frac{1}{\sqrt{2N}}\sum_n R^3_{\alpha n}$	CH wagging
	$S_4=\frac{1}{\sqrt{2N}}\sum_n R^4_{\alpha n}$	Deformation 1
	$S_5=\frac{1}{\sqrt{2N}}\sum_n R^5_{\alpha n}$	Deformation 2
	$S_6=\frac{1}{\sqrt{2N}}\sum_n R^1_{\beta n}$	CH_2 symmetric stretching
	$S_7=\frac{1}{\sqrt{2N}}\sum_n R^2_{\beta n}$	CH_2 scissor
	$S_8=\frac{1}{\sqrt{2N}}\sum_n R^3_{\beta n}$	CCC bending
	$S_9=\frac{1}{\sqrt{2N}}\sum_n R^4_{\beta n}$	CH_2 twisting

Table IV. (continued)

	$S_{10}=\frac{1}{\sqrt{4N}}\sum_n(R^8_{\alpha n}+R^8_{\beta n})$	CC stretching
	$S_{11}=\frac{1}{\sqrt{4N}}\sum_n(-1)^n(R^9_{\alpha n}+R^9_{\beta n})$	Internal rotation
$A_2(A'')$	$S_{12}=\frac{1}{\sqrt{2N}}\sum_n(-1)^nR^6_{\alpha n}$	CH wagging
	$S_{13}=\frac{1}{\sqrt{2N}}\sum_n(-1)^nR^7_{\alpha n}$	CCl wagging
	$S_{14}=\frac{1}{\sqrt{2N}}\sum_n(-1)^nR^1_{\beta n}$	CH_2 symmetric stretching
	$S_{15}=\frac{1}{\sqrt{2N}}\sum_n(-1)^nR^2_{\beta n}$	CH_2 scissor
	$S_{16}=\frac{1}{\sqrt{2N}}\sum_n(-1)^nR^3_{\beta n}$	CCC bending
	$S_{17}=\frac{1}{\sqrt{2N}}\sum_n(-1)^nR^4_{\beta n}$	CH_2 twisting
	$S_{18}=\frac{1}{\sqrt{4N}}\sum_n(-1)^n(R^8_{\alpha n}+R^8_{\beta n})$	CC stretching
	$S_{19}=\frac{1}{\sqrt{4N}}\sum_n(R^9_{\alpha n}+R^9_{\beta n})$	Internal rotation
$B_1(A')$	$S_{20}=\frac{1}{\sqrt{2N}}\sum_n R^6_{\alpha n}$	CH wagging
	$S_{21}=\frac{1}{\sqrt{2N}}\sum_n R^7_{\alpha n}$	CCl wagging
	$S_{22}=\frac{1}{\sqrt{2N}}\sum_n R^5_{\beta n}$	CH_2 antisymmetric stretching
	$S_{23}=\frac{1}{\sqrt{2N}}\sum_n R^6_{\beta n}$	CH_2 wagging
	$S_{24}=\frac{1}{\sqrt{2N}}\sum_n R^7_{\beta n}$	CH_2 rocking
	$S_{25}=\frac{1}{\sqrt{4N}}\sum_n(R^8_{\alpha n}-R^8_{\beta n})$	CC stretching
	$S_{26}=\frac{1}{\sqrt{4N}}\sum_n(-1)^n(R^9_{\alpha n}-R^9_{\beta n})$	Internal rotation
$B_2(A'')$	$S_{27}=\frac{1}{\sqrt{2N}}\sum_n(-1)^nR^1_{\alpha n}$	CH stretching
	$S_{28}=\frac{1}{\sqrt{2N}}\sum_n(-1)^nR^2_{\alpha n}$	CCl stretching
	$S_{29}=\frac{1}{\sqrt{2N}}\sum_n(-1)^nR^3_{\alpha n}$	CH bending
	$S_{30}=\frac{1}{\sqrt{2N}}\sum_n(-1)^nR^4_{\alpha n}$	Deformation 1
	$S_{31}=\frac{1}{\sqrt{2N}}\sum_n(-1)^nR^5_{\alpha n}$	Deformation 2
	$S_{32}=\frac{1}{\sqrt{2N}}\sum_n(=1)^nR^5_{\beta n}$	CH_2 antisymmetric stretching
	$S_{33}=\frac{1}{\sqrt{2N}}\sum_n(-1)^nR^6_{\beta n}$	CH_2 wagging
	$S_{34}=\frac{1}{\sqrt{2N}}\sum_n(-1)^nR^7_{\beta n}$	CH_2 rocking
	$S_{35}=\frac{1}{\sqrt{4N}}\sum_n(-1)^n(R^8_{\alpha n}-R^8_{\beta n})$	CC stretching
	$S_{36}=\frac{1}{\sqrt{4N}}\sum_n(R^9_{\alpha n}-R^9_{\beta n})$	Internal rotation

Force Constants

We used a modified Urey—Bradley force field which is given in Table V. Besides the conventional Urey—Bradley force constants represented by K, H, F, and κ[7], some valence force constants are included. The constant p(CC, CC) represents the interaction term between the stretching of two adjacent CC bonds. Likewise p(CH, CH) is put between the two CH-stretching coordinates. The definition of t, t', g, and g' is given in Figure 2. Numerical values of force constants were adjusted by the method of trial and error in order to get a good agreement between the observed and calculated freqaencies. In doing this, great deviations of the values from those of CH_3CH_2Cl, $CH_3CHClCH_3$, and $(CH_3)_3CCl$ were avoided to keep the transferability of force constants among similar molecules. The force constants related to the methylene group may be transformed into the local-symmetry force constants given in ref 2. The internal-rotation constant Y used here for PVC is slightly different from that of polyethylene.

Table V. Force constants[a]

Urey—Bradly force constants[a]			
K(C—C)	2.541	H(Cl—C—C)	0.130
K(C—H) of CH_2	4.122	F(C...C)	0.300
K(C—H) of CHCl	4.072	F(H...H)	0.215
K(C—Cl)	1.450	F(H...C)	0.475
H(C—C—C)	0.280	F(H...Cl)	0.720
H(H—C—H)	0.347	F(Cl...C)	0.600
H(H—C—C)	0.219	κ of CH_2	−0.011
H(H—C—Cl)	0.055	κ of CHCl	0.070
Non—Urey—Bradley force constants[b]			
Y	0.110	g'	−0.005
p(CH, CH)	−0.116	f(scis)	0.007
p(CC, CC)	−0.078	f(wag)	−0.013
t	0.096	f(rock)	0.013
g	−0.036	f(twist)	−0.033
t'	−0.011		

[a] Units are md/Å for K, H, F, and p and md·Å for κ, Y, t, g, t', g', and f.

[b] As for the definitions of Y, p, t, g', see the text and Figure 2. The constant represented by f is the correction term which should be added to the respective diagonal element of local-symmetry force field.

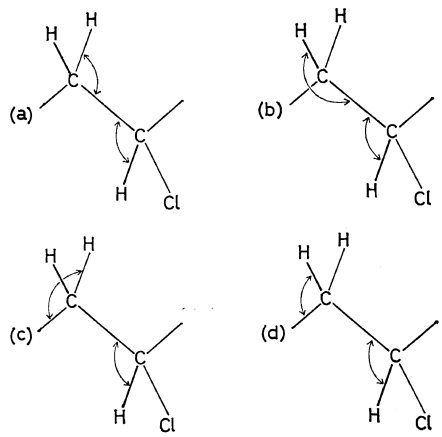

Figure 2. The force constants represented by t, g, t' and g' correspond, respectively, to the interactions between the angles shown in (a), (b), (c), and (d).

RESULTS AND DISCUSSION

The results of calculation and our assignments of observed frequencies are shown in Tables VI—XI. Most of the crystalline bands reported in ref 4 could be assigned. Some very weak crystalline bands and amorphous ones were left unassigned.

PVC

The study of dichroism for the films with various draw-ratios has established the symmetry assignments of most of the crystalline bands.[3]

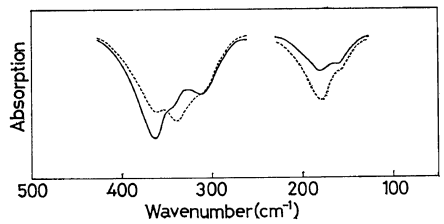

Figure 3. Far-infrared spectra of PVC. The solid and broken curves indicate perpendicular and parallel absorptions, respectively.

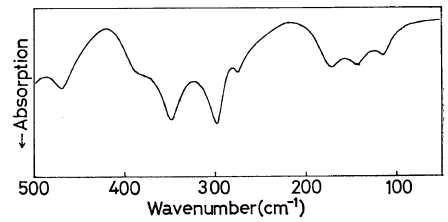

Figure 4. Far-infrared spectrum of PVC-β,β-d_2.

The A_1 bands are always polarized perpendicularly to the drawing direction, and the B_1 bands are parallel at high draw-ratios, whereas the dichroism of the B_2 bands changes from parallel to perpendicular with the degree of drawing. However, there are a few bands which do not exhibit definite dichroic behavior because of the overlapping of other bands or of their very weak intensities. For instance, the band at 1090 cm^{-1} shows neither clear parallel dichroism at high draw-ratios nor the change of dichroism from parallel to perpendicular. This band is a shoulder of the 1105 cm^{-1} band which is an A_1 band. Probably there is also some contribution from the amorphous part in this frequency region. The band at about 1030 cm^{-1} is very weak and the dichroism is not determined. Having such difficulties in assigning these two bands experimentally to proper symmetry species, we resort to the results of calculation and assign the 1090-

Table VI. Observed and calculated frequencies (in cm^{-1}), potential energy distributions, and band assignments of PVC

Mode		Obsd frequency Intensity Dichroism[a]	Calcd frequency	PED[b]	Assignment
A_1	ν_1	2970 mw ⊥	2960	$-S_1(97)$	CH str.
	ν_2	2910 s ⊥	2893	$+S_6$	CH_2 sym. str.
	ν_3	1428 s ⊥	1445	$+S_7(100)$	CH_2 scis.
	ν_4	1338 ms ⊥	1322	$-S_9(47)+S_3(45)$	CH_2 twist., CH bend.
	ν_5		1169	$-S_3(46)-S_9(39)-S_{10}(16)$	CH bend., CH_2 twist.
	ν_6	1105 m ⊥	1122	$-S_{10}(46)+S_8(18)+S_5(16)$	Skeletatl
	ν_7	640 s ⊥	639	$+S_2(95)+S_4(24)$	CCl str.
	ν_8	364 m ⊥	349	$+S_4(57)-S_2(16)+S_5(15)$	CCl bend.
	ν_9		54	$+S_{11}(95)$	Torsion
A_2	ν_{10}		2896	$+S_{14}(101)$	CH_2 sym. str.
	ν_{11}		1440	$+S_{15}(101)$	CH_2 scis.
	ν_{12}		1351	$+S_{12}(73)-S_{17}(15)$	CH wag.
	ν_{13}		1133	$+S_{17}(85)+S_{12}(25)$	CH_2 twist.
	ν_{14}		1025	$+S_{18}(99)$	CC str.
	ν_{15}		549	$+S_{16}(65)+S_{13}(30)$	CCC bend.
	ν_{16}		127	$+S_{13}(67)-S_{16}(34)$	CCl wag.
B_1	ν_{17}		2949	$-S_{22}(101)$	CH_2 antisym. str.
	ν_{18}	1387 w //	1404	$+S_{20}(57)-S_{23}(31)+S_{25}(27)$	CH wag.
	ν_{19}	1230 mw //	1233	$+S_{23}(70)+S_{20}(34)$	CH_2 wag.
	ν_{20}	1090 sh	1076	$+S_{25}(78)$	CC str.
	ν_{21}	835 mw //	835	$-S_{24}(89)$	CH_2 rock.
	ν_{22}	340 sh //	347	$+S_{21}(79)+S_{26}(15)$	CCl wag.
	ν_{23}		117	$-S_{26}(81)$	Torsion
B_2	ν_{24}	2970 mw ⊥	2962	$-S_{27}(70)+S_{32}(31)$	CH str.
	ν_{25}	2930 w ⊥	2944	$-S_{32}(70)-S_{27}(32)$	CH_2 antisym. str.
	ν_{26}	1355 w ⊥	1311	$+S_{33}(99)$	CH_2 wag.
	ν_{27}	1258 s ⊥	1278	$+S_{29}(87)$	CH bend.
	ν_{28}	1030 vw ⊥	1022	$-S_{35}(78)-S_{34}(20)$	CC str.
	ν_{29}	960 ms ⊥	1002	$+S_{34}(44)-S_{35}(28)$	CH_2 rock.
	ν_{30}	604 s ⊥	619	$-S_{28}(92)-S_{31}(24)$	CCl str.
	ν_{31}	490 w	476	$+S_{30}(76)$	Deform. 1
	ν_{32}	312 w ⊥	310	$-S_{31}(63)$	Deform. 2

[a] Observed data are taken from ref 3 and 4, and Figure 3.

[b] Potential-energy distribution (PED) is indicated by the number in parenthesis following symmetry coordinate. The values of PED given here are not normalized to 100. The sign of corresponding element of eigenvector is also shown.

and 1030-cm^{-1} bands to ν_{20} (CC-stretching mode of B_1, ν_{calc}=1076 cm^{-1}) and ν_{28} (CC-stretching mode of B_2, ν_{calc}=1022 cm^{-1}), respectively. The 1105-cm^{-1} band is undoubtedly the skeletal mode of A_1 (ν_6, ν_{calc}=1122 cm^{-1}). Such assignments have some analogy to the skeletal modes of polyethylene. In the case of polyethylene[2] $\nu_4(0)$ (A_1-type mode), $\nu_4(\pi/2)$ (B_2-type mode), $\nu_4(\pi)$ (B_1-type mode) are located, respectively, at 1131 cm^{-1} about 1000 cm^{-1}, and 1061 cm^{-1}. The mode ν_4 ($\pi/2$) of polyethylene, which is degenerate, splits into ν_{14} (A_2, ν_{calc}=1025 cm^{-1}) and ν_{28} (B_2, ν_{calc}=1022 cm^{-1}) in the case of PVC. Formerly a parallel band at 1122 cm^{-1} was assigned to ν_{20} (B_1 CC-stretching mode)[1]. However, the intensity of this band decreases in the spectrum of the urea-complex PVC and, therefore, this band is associated with the amorphous part[4]. The assignment of the 1195-cm^{-1} band to ν_{20}[4] does not seem to have a strong basis to support it.

The assignment of the 1338-cm^{-1} band has been a subject of some discussions[3]. Our present calculation indicates that this band should be assigned to ν_4, in which the CH_2-twisting and

Table VII. Observed and calculated frequencies (in cm^{-1}), potential energy distributions, and band assignments of PVC-α-d_1

Mode		Obsd frequency Intensity Dichroism[a]		Calcd frequency	PED	Assignment
A_1	ν_1	2910 s	⊥	2897	$-S_6(101)$	CH_2 sym. str.
	ν_2	2200 w	⊥	2160	$-S_1(102)$	CD str.
	ν_3	1430 s	⊥	1444	$-S_7(101)$	CH_2 scis.
	ν_4	1297 ms	⊥	1262	$+S_9(86)$	CH_2 twist.
	ν_5	1110 vw		1133	$+S_{10}(62)-S_8(24)-S_5(20)$	Skeletal
	ν_6	888 mw	⊥	872	$-S_3(97)$	CD bend.
	ν_7	625 s	⊥	630	$-S_2(94)-S_4(22)$	CCl str.
	ν_8	358	⊥	344	$-S_4(58)-S_5(15)+S_2(15)$	CCl bend.
	ν_9			54	$-S_{11}(95)$	Torsion
A_2	ν_{10}			2896	$+S_{14}(101)$	CH_2 sym. str.
	ν_{11}			1440	$+S_{15}(101)$	CH_2 scis.
	ν_{12}			1210	$-S_{17}(75)$	CH_2 twist.
	ν_{13}			1073	$+S_{18}(73)+S_{12}(28)+S_{17}(19)$	CC str.
	ν_{14}			913	$+S_{12}(51)-S_{18}(29)$	CD wag.
	ν_{15}			514	$-S_{16}(60)-S_{13}(29)+S_{12}(15)$	CCC bend.
	ν_{16}			127	$-S_{13}(67)+S_{16}(34)$	CCl wag.
B_1	ν_{17}			2949	$+S_{22}(101)$	CH_2 antisym. str.
	ν_{18}	1353 ms	//	1331	$+S_{23}(78)-S_{25}(48)$	CH_2 wag.
	ν_{19}	1160 vw		1126	$-S_{25}(39)-S_{23}(29)-S_{20}(26)$	CC str.
	ν_{20}	1000 vw	//	989	$-S_{24}(35)-S_{25}(25)+S_{20}(23)$	CH_2 rock.
	ν_{21}	769 m	//	765	$-S_{24}(57)-S_{20}(45)$	CH_2 rock, CD wag.
	ν_{22}	345	//	347	$-S_{21}(79)-S_{26}(15)$	CCl wag.
	ν_{23}			115	$-S_{26}(81)$	Torsion
B_2	ν_{24}	2935 mw		2950	$-S_{32}(101)$	CH_2 antisym. str.
	ν_{25}	2200 w	⊥	2160	$-S_{27}(103)$	CD str.
	ν_{26}	1360 ms	⊥	1308	$+S_{33}(101)$	CH_2 wag.
	ν_{27}	1080 s	⊥	1100	$+S_{34}(46)-S_{29}(32)$	CH_2 rock., CD bend.
	ν_{28}	1020 vw	⊥	1015	$+S_{35}(95)$	CC str.
	ν_{29}	835 w	⊥	846	$-S_{29}(67)-S_{34}(19)$	CD bend.
	ν_{30}	598 s	⊥	614	$-S_{28}(94)-S_{31}(22)$	CCl str.
	ν_{31}	473		469	$+S_{30}(77)$	Deform. 1
	ν_{32}	297	⊥	305	$-S_{31}(64)$	Deform. 2

[a] Observed data are taken from ref 4 and 8.

CH-bending coordinates are mixed almost equally. Though the amount of mixing may vary depending on the assumed force field, it is certain that they are mixed in ν_4.

The calculated frequency of ν_{26} (CH_2-wagging mode of B_2) is lower than the observed by about 40 cm^{-1}, whereas the agreement between the observed and calculated frequencies is much better for ν_{18} and ν_{19} (CH- and CH_2-wagging modes of B_1). This suggests that the force field used here is still capable of some improvement.

Assignments of low-frequency vibrations are also important. In Figure 3 the far-infrared spectrum of a highly sydiotactic sample is shown. The bands at 364, 340, and 312 cm^{-1} may be assigned, respectively, to ν_8 (CCl bending of A_1), ν_{22} (CCl bending of B_1), and ν_{32} (CCl bending of B_2) in accordance with the results of calculation and dichroism measurements. We have tentatively taken the 490-cm^{-1} band to ν_{31} (skeletal-deformation vibration of B_2), though there remains some doubt about its polarization. The parallel band at 180 cm^{-1} raises a question. From the single-chain analysis, only ν_{23} (internal rota-

Table VIII. Observed and calculated frequencies (in cm^{-1}), potential energy distributions, and band assignments of PVC-β,β-d_2

Mode		Obsd frequency Intensity Dichroism[a]		Calcd frequency	PED	Assignment
A_1	ν_1	2962 w	⊥	2956	$+S_1(102)$	CH str.
	ν_2	2112 w	⊥	2099	$-S_6(101)$	CD_2 sym. str.
	ν_3	1252 vs	⊥	1255	$+S_3(96)$	CH bend.
	ν_4	1105 m	⊥	1146	$+S_{10}(51)+S_7(27)-S_5(16)$	Skeletal
	ν_5	1020 w	⊥	1020	$-S_7(73)$	CD_2 scis.
	ν_6	955 w	⊥	943	$+S_9(75)$	CD_2 twist.
	ν_7	599 s	⊥	592	$-S_2(85)+S_9(19)-S_4(17)$	CCl str.
	ν_8	348 m		340	$-S_4(57)-S_5(16)$	CCl bend.
	ν_9			54	$+S_{11}(95)$	Torsion
A_2	ν_{10}			2098	$+S_{14}(101)$	CD_2 sym. str.
	ν_{11}			1318	$-S_{12}(93)$	CH wag.
	ν_{12}			1099	$+S_{15}(66)+S_{18}(49)$	CD_2 scis., CC str.
	ν_{13}			969	$+S_{18}(54)-S_{15}(33)$	CC str., CD_2 scis.
	ν_{14}			821	$+S_{17}(99)$	CD_2 twist.
	ν_{15}			527	$+S_{16}(63)+S_{13}(29)$	CCC bend.
	ν_{16}			127	$+S_{13}(67)-S_{16}(34)$	CCl wag.
B_1	ν_{17}			2185	$-S_{22}(101)$	CD_2 antisym. str.
	ν_{18}	1325 w	//	1365	$-S_{20}(77)-S_{25}(30)$	CH wag.
	ν_{19}	1167 m	//	1140	$+S_{25}(67)-S_{23}(30)-S_{20}(18)$	CC str.
	ν_{20}	885 sh	//	869	$-S_{23}(69)-S_{25}(15)$	CD_2 wag.
	ν_{21}	709 vw	//	685	$-S_{24}(88)$	CD_2 rock.
	ν_{22}	298 m		303	$-S_{21}(75)$	CCl wag.
	ν_{23}			109	$-S_{26}(86)$	Torsion
B_2	ν_{24}	2962 w	⊥	2956	$-S_{27}(102)$	CH str.
	ν_{25}	2210 w	⊥	2185	$-S_{32}(101)$	CD_2 antisym. str.
	ν_{26}	1252 vs	⊥	1267	$-S_{29}(96)$	CH bend.
	ν_{27}			1102	$-S_{33}(65)+S_{35}(61)$	CD_2 wag., CC str.
	ν_{28}	955 w	⊥	947	$-S_{35}(49)-S_{33}(25)$	CC str., CD_2 wag.
	ν_{29}	900 s	⊥	912	$+S_{34}(49)+S_{28}(22)+S_{30}(17)$	CD_2 rock.
	ν_{30}	565 s	⊥	566	$-S_{28}(81)$	CCl str.
	ν_{31}	390 w		412	$-S_{30}(58)+S_{31}(18)+S_{34}(16)$	Deform. 1
	ν_{32}	275 w		280	$+S_{31}(57)$	Deform. 2

[a] Observed data are taken from ref 5 and Figure 4.

tion of B_1) is left to explain this band. The calculated frequency of ν_{23} (117 cm^{-1}) is, however, considerably lower than the observed. It is likely that this absorption arises from a mode in which the internal rotation is coupled with a lattice vibration.

According to the selection rule for the C_{2v} symmetry, the A_2 vibrations can be Raman-active while they are infrared-inactive. In the observed Raman spectrum[6], however, it is rather difficult to pick up the bands which are clearly due to the A_2 vibrations. On the other hand, the results of depolarization measurements of Raman bands are consistent with the assignments of the bands at 2910, 1428, 1338, 640 and 364 cm^{-1} to the A_1 species.

PVC-α-d_1

The first problem is the assignments of the bands at 1360 (⊥), 1353 (//), and 1297 (⊥) cm^{-1}. Krimm, *et al.*,[4] assigned these bands, respectively, to the CH_2 wagging of B_2, the CH_2 wagging of B_1, and the CH_2 twisting of A_1. These assignments are supported by our calculation. We note that, just like the case of PVC, the cal-

Table IX. Observed and calculated frequencies (in cm^{-1}), potential energy distributions, and band assignments of PVC-d_3

Mode		Obsd frequency	Intensity	Dichroism[a]	Calcd frequency	PED	Assignment
A_1	ν_1	2160	m	⊥	2163	$-S_1(97)$	CD str.
	ν_2	2110	mw	⊥	2095	$+S_6(96)$	CD_2 sym. str.
	ν_3	1118	ms	⊥	1148	$-S_{10}(54)-S_7(22)+S_8(21)+S_5(19)$	Skeletal
	ν_4	1040	w	⊥	1049	$-S_7(55)+S_3(22)$	CD_2 scis.
	ν_5				982	$+S_9(42)-S_7(22)$	CD_2 twist.
	ν_6	865	vw		834	$-S_3(67)-S_9(26)$	CD bend.
	ν_7	595	s	⊥	589	$-S_2(86)+S_9(18)-S_4(17)$	CCl str.
	ν_8	344		⊥	335	$-S_4(58)-S_5(16)$	CCl bend.
	ν_9				53	$+S_{11}(95)$	Torsion
A_2	ν_{10}				2098	$-S_{14}(101)$	CD_2 sym. str.
	ν_{11}				1118	$-S_{18}(72)-S_{15}(25)-S_{12}(24)$	CC str.
	ν_{12}				1064	$-S_{15}(61)+S_{12}(29)$	CD_2 scis.
	ν_{13}				900	$-S_{18}(35)+S_{12}(20)$	CC str., CD wag.
	ν_{14}				806	$-S_{17}(84)-S_{12}(19)$	CD_2 twist.
	ν_{15}				498	$+S_{16}(59)+S_{13}(29)$	CCC bend.
	ν_{16}				127	$-S_{13}(67)+S_{16}(34)$	CCl wag.
B_1	ν_{17}				2184	$+S_{22}(102)$	CD_2 antisym. str.
	ν_{18}	1256	mw	//	1252	$+S_{25}(85)-S_{23}(27)+S_{20}(23)$	CC str.
	ν_{19}	940	m	//	951	$-S_{20}(60)-S_{23}(24)$	CD wag.
	ν_{20}				863	$+S_{23}(56)+S_{25}(19)$	CD_2 wag.
	ν_{21}	670	mw		656	$-S_{24}(77)-S_{20}(19)$	CD_2 rock.
	ν_{22}	300		//	303	$-S_{21}(75)$	CCl wag.
	ν_{23}				107	$-S_{26}(85)$	Torsion
B_2	ν_{24}	2230	m	⊥	2186	$+S_{32}(96)$	CD_2 antisym. str.
	ν_{25}	2160	mw	⊥	2158	$-S_{27}(98)$	CD str.
	ν_{26}				1102	$+S_{33}(64)-S_{35}(63)$	CD_2 wag., CC str.
	ν_{27}	1010	ms	⊥	1040	$+S_{29}(54)-S_{34}(22)-S_{28}(17)$	CD bend.
	ν_{28}				934	$+S_{35}(39)+S_{33}(21)$	CC str.
	ν_{29}	792	ms	⊥	802	$+S_{29}(45)+S_{34}(22)$	CD bend.
	ν_{30}	560	s	⊥	565	$-S_{28}(82)$	CCl str.
	ν_{31}	390		⊥	405	$-S_{30}(59)+S_{31}(17)+S_{34}(16)$	Deform. 1
	ν_{32}	275			277	$+S_{31}(59)$	Deform. 2

[a] Observed data are taken from ref 4 and 8.

culated frequency of the CH_2-wagging mode of B_2 (1308 cm^{-1}) is considerably lower than the observed (1360 cm^{-1}). The strong absorption at 1080 cm^{-1} may be assigned to ν_{27}, in which the CH_2-rocking and CD-bending coordinates are coupled.

It seems reasonable from the results of calculation to associate the bands at 1160, 1110, and 1020 cm^{-1} to $\nu_{19}(B_1)$, $\nu_5(A_1)$, and $\nu_{28}(B_2)$, respectively, though the dichroism of the former two bands is ambiguous. The parallel bands at 1000 and 769 cm^{-1} may be assigned to ν_{20} and ν_{21}, both of which have the components of CH_2-rocking and CD-wagging modes.

The CCl-stretching modes are shifted to slightly lower frequencies by α-deuteration. The crystalline bands at 625 and 598 cm^{-1} are assigned to $\nu_7(A_1)$ and $\nu_{30}(B_2)$, respectively. The 358 cm^{-1} band may be assigned to ν_8 (CCl-bending of A_1). The 345 cm^{-1} band is assigned to ν_{22} (CCl wagging of B_1) from its parallel dichroism. The 297 cm^{-1} band is undoubtedly due to ν_{32} (CCl-bending mode of B_2).

Table X. Observed and calculated frequencies (in cm^{-1}), potential energy distributions, and band assignments of PVC-β-d_1

Mode		Obsd frequency	Intensity	Dichroism[a]	Calcd frequency	PED	Assignment
A'	ν_1	2980	m	⊥	2959	$-S_1(94)$	CH(α) str.
	ν_2	2920	ms	⊥	2922	$-S_{22}(51)+S_6(43)$	CH(β) str.
	ν_3	2170	w	⊥	2141	$-S_6(55)-S_{22}(46)$	CD str.
	ν_4	1372	mw	⊥	1391	$+S_{20}(59)+S_{25}(26)-S_{23}(19)$	CH(α) wag.
	ν_5	1292	vs	⊥	1309	$-S_7(50)+S_3(25)$	CH(β) bend., CH(α) bend.
	ν_6	1263	vs	⊥	1269	$+S_7(50)+S_3(25)$	CH(β) bend., CH(α) bend.
	ν_7	1210	mw	//	1195	$-S_{23}(37)+S_3(36)-S_{20}(18)$	CH(β) wag.
	ν_8	1140	mw	//	1127	$+S_{10}(44)-S_{25}(20)-S_8(17)$	Skeletal
	ν_9	1090	mw	⊥	1095	$-S_{25}(43)+S_9(16)$	CC str.
	ν_{10}	872	m		904	$+S_{23}(38)+S_9(29)$	CD wag.
	ν_{11}	747	mw	//	733	$-S_{24}(85)$	CHD rock.
	ν_{12}	622	s	⊥	613	$+S_2(87)+S_4(20)$	CCl str.
	ν_{13}	353		⊥	346	$+S_4(53)$	CCl bend.
	ν_{14}	318		//	321	$-S_{21}(71)$	CCl wag.
	ν_{15}				113	$+S_{26}(83)$	Torsion
	ν_{16}				54	$-S_{11}(95)$	Torsion
A''	ν_{17}	2980	m	⊥	2957	$-S_{27}(98)$	CH(α) str.
	ν_{18}	2920	ms	⊥	2923	$+S_{32}(53)-S_{14}(45)$	CH(β) str.
	ν_{19}	2170	w	⊥	2140	$+S_{14}(55)+S_{32}(46)$	CD str.
	ν_{20}	1340	mw	⊥	1344	$+S_{12}(68)$	CH(α) wag.
	ν_{21}	1292	vs	⊥	1304	$+S_{15}(63)-S_{29}(24)$	CH(β) bend., CH(α) bend.
	ν_{22}	1240	vs	⊥	1260	$+S_{29}(63)+S_{15}(26)$	CH(α) bend., CH(β) bend.
	ν_{23}				1237	$+S_{33}(57)-S_{12}(22)$	CH(β) wag.
	ν_{24}				1032	$-S_{35}(74)+S_{18}(21)$	CC str.
	ν_{25}				1020	$+S_{18}(71)+S_{35}(18)$	CC str.
	ν_{26}	904	ms	⊥	929	$+S_{34}(47)+S_{30}(20)$	CHD rock.
	ν_{27}	872	m		888	$-S_{17}(57)-S_{33}(15)$	CD wag.
	ν_{28}	580	s	⊥	589	$-S_{28}(81)-S_{31}(17)$	CCl str.
	ν_{29}				538	$-S_{16}(61)-S_{13}(28)$	CCC bend.
	ν_{30}	407			436	$+S_{30}(63)$	Deform. 1
	ν_{31}				294	$-S_{31}(60)$	Deform. 2
	ν_{32}				127	$+S_{13}(67)$	CCl wag.

[a] Observed data are taken from ref 4 and 8.

PVC-β,β-d_2

The parallel bands at 1325, 1167, 885, and 709 cm^{-1} may be explained by ν_{18}, ν_{19}, ν_{20}, and ν_{21}.

The strong band at 1252 cm^{-1} is due to the two CH-bending modes, $\nu_3(A_1)$ and $\nu_{26}(B_2)$. In this polymer the CH bending mode is free from the coupling with other modes. As a result the calculated frequencies of ν_3 and ν_{26} are not much different. The band at 1105 cm^{-1} may be assigned to ν_4 (skeletal mode of A_1). The 1020 cm^{-1} band is certainly due to ν_5 (CD_2-scissor mode of A_1). The strong band at 900 cm^{-1} arises from ν_{29} (CD_2-rocking mode of B_2). The corresponding band is found at 960 cm^{-1} in the spectrum of PVC. There is no simple corresponding band in the spectrum of PVC-α-d_1 because of the coupling between CH_2-rocking and CD-bending modes. This provides a good example of the difficulties in predicting the frequencies of deuterated compounds without normal-coordinate treatments.

The CCl stretching frequencies are shifted down much more by β-deuteration ($\nu(A_1)$ is shifted

Table XI. Observed and calculated frequencies (in cm^{-1}), potential energy distributions, and band assignments of PVC-α,β-d_2

Mode		Obsd frequency	Intensity	Dichroism[a]	Calcd frequency	PED	Assignment
A'	ν_1	2920	ms	⊥	2924	$+S_{22}(55)+S_6(46)$	CH str.
	ν_2	2208	w	⊥	2165	$-S_1(83)$	CD(α) str.
	ν_3	2180	w	⊥	2135	$-S_6(46)+S_{22}(37)-S_1(19)$	CD(β) str.
	ν_4	1330	m	⊥	1312	$-S_{23}(51)+S_{25}(40)-S_9(16)$	CHD wag., CC str.
	ν_5	1282	s	⊥	1291	$+S_7(87)$	CHD scis.
	ν_6	1185	mw	⊥	1181	$-S_{25}(39)-S_9(34)$	CC str., CHD twist.
	ν_7	1115	vw		1123	$-S_{10}(53)+S_8(21)+S_5(17)$	Skeletal
	ν_8	962	mw	⊥	973	$-S_{20}(39)-S_{23}(28)$	CD(α) wag., CHD wag.
	ν_9	938	mw	⊥	917	$-S_{25}(21)-S_3(18)$	CC str., CD(α) bend.
	ν_{10}	816	vw		843	$-S_3(63)-S_9(22)$	CD(α) bend.
	ν_{11}	705	mw	//	695	$-S_{24}(69)-S_{26}(25)$	CHD rock.
	ν_{12}	615	s	⊥	607	$-S_2(87)-S_4(19)$	CCl str.
	ν_{13}	352			342	$+S_4(53)$	CCl bend.
	ν_{14}	316			320	$-S_{21}(69)$	CCl wag.
	ν_{15}				111	$+S_{26}(83)-S_{20}(39)$	Torsion
	ν_{16}				53	$+S_{11}(95)$	Torsion
A''	ν_{17}	2920	ms	⊥	2924	$+S_{32}(55)+S_{14}(46)$	CH str.
	ν_{18}	2208	w	⊥	2160	$+S_{27}(99)$	CD(α) str.
	ν_{19}	2180	w	⊥	2139	$-S_{14}(53)+S_{32}(45)$	CD(β) str.
	ν_{20}	1310	vw		1294	$-S_{15}(90)$	CHD scis.
	ν_{21}	1238	w	⊥	1270	$-S_{33}(70)-S_{17}(25)$	CH(β) wag.
	ν_{22}	1115	vw		1105	$+S_{18}(56)+S_{12}(38)$	CC str., CD wag.
	ν_{23}	1025	s	⊥	1054	$+S_{29}(42)+S_{35}(34)-S_{34}(16)$	CD bend., CC str.
	ν_{24}	1058	w		1023	$-S_{35}(48)-S_{17}(16)$	CC str.
	ν_{25}	918	vw		919	$+S_{18}(28)-S_{12}(18)$	CC str., CD wag.
	ν_{26}	880	w	⊥	879	$-S_{17}(40)-S_{12}(24)$	CHD twist.
	ν_{27}	802	m	⊥	807	$+S_{29}(42)+S_{34}(18)$	CD(μ) bend., CHD rock.
	ν_{28}	580	s	⊥	585	$+S_{28}(85)+S_{31}(17)$	CCl str.
	ν_{29}				507	$-S_{16}(58)-S_{13}(28)$	CCC bend.
	ν_{30}	403			429	$-S_{30}(64)$	Deform. 1
	ν_{31}	288			290	$-S_{31}(62)$	Deform. 2
	ν_{32}				127	$-S_{13}(67)+S_{16}(34)$	CCl wag., CCC bend.

[a] Observed data are taken from ref 4 and 8.

from 640 to 599 cm^{-1} and $\nu(B_2)$ from 604 to 565 cm^{-1}) than by α-deuteration ($\nu(A_1)$ from 640 to 625 cm^{-1}, $\nu(B_2)$ from 604 to 598 cm^{-1}). The calculation follows satisfactorily these experimental findings.

Figure 4 shows the low-frequency spectrum of this polymer, which we measured for the sample provided by Enomoto. The bands at 390, 348, 298, and 275 cm^{-1} may be assigned to ν_{31}, ν_8, ν_{22}, and ν_{32}, respectively. It is noted that ν_{22} is greatly affected by the β-deuteration. Three bands are found in the region below 200 cm^{-1}. Their origins are ambiguous, however. Probably the band at 172 cm^{-1} is analogous to the 187-cm^{-1} band of PVC.

PVC-d_3

Assignments of bands having major intensities may be made without much difficulty in reference to the results of our calculations. We have changed some of our former assignments[1]. For instance, the strong band at 1010 cm^{-1} is now assigned to ν_{27} (a B_2 mode in which the CD-bending, CD_2-rocking, and CCl-stretching coordinates are mixed) rather than to ν_4 (an A_1 mode which is mainly composed of the CD_2-scissor and CD-bending coordinates). To the latter the shoulder band at 1040 cm^{-1} is assigned. It seems more reasonable to associate a mode having a large CD-bending (B_2) component to a band with greater intensity, since in the PVC spectrum ν_{27} (almost pure CH-bending mode of B_2) has the strongest intensity.

PVC-β-d_1 and PVC-α,β-d_2

Assignments are a little more difficult for PVC-β-d_1 and PVC-α,β-d_2, because the symmetry of these polymers is not higher than C_s. For the C_{2v} structure we could pick up the B_1 bands easily as they should show parallel dichroism. For the C_s structure the transition moments of the A' modes are limited in the skeletal plane, whereas those of the A'' modes are perpendicular to the plane. The problem is that there is no further prediction regarding the direction of the A' transition moments. Under such circumstances it is reasonable to expect that, if an A' normal coordinates is made up almost solely of the B_1 symmetry coordinates of C_{2v}, the band due to the normal mode would show parallel dichroism. For example, ν_{11} (ν_{calc}=733 cm^{-1}) and ν_{14} (ν_{calc}=321 cm^{-1}) of PVC-β-d_1 are mostly composed of the B_1 coordinates. Parallel bands at 747 and 318 cm^{-1} may, therefore, be assigned to them. It appears, however, that there is no simple way of predicting the direction of the transition moment when considerable coupling of the A_1 and B_1 modes takes place in a normal mode.

In the spectrum of PVC-α,β-d_2 no definitely parallel band has been obsereed in the NaCl region except for the 705-cm^{-1} band. This fact suggests that the coupling of the A_1 and B_1 coordinates in the A' species of this polymer has a great effect on the direction of the transition moment.

In conclusion we may say that it was possible to assign most of the main bands of deuterated polymers reasonably well with the aid of the calculations. This increases the reliability of band assignments of nondeuterated polymer.

Acknowledgment. We are greatful to Dr. S. Enomoto of Kureha Chemical Industry Co. for giving us the sample of PVC-β,β-d_2.

REFERENCES

1. T. Shimanouchi and M. Tasumi, *Bull. Chem. Soc. Japan*, **34**, 359 (1961).
2. (a) M. Tasumi, T. Shimanouchi, and T. Miyazawa, *J. Mol. Spectrosc.*, **9**, 261 (1962); **11**, 422 (1963); (b) M. Tasumi and T. Shimanouchi, *J. Chem. Phys.*, **43**, 1245 (1965).
3. M. Tasumi and T. Shimanouchi, *Spectrochim. Acta*, **17**, 731 (1961).
4. S. Krimm, V. L. Folt, J. J. Shipman, and A. R. Berens, *J. Polym. Sci., Part A*, **1**, 2621 (1963).
5. S. Enomoto, M. Asahina, and S. Satoh, *J. Polym. Sci., Part A-1*, **4** 1373 (1966).
6. J. L. Koenig and D. Druesedow, *J. Polym. Sci., Part A-2*, **7**, 1075 (1969).
7. T. Shimanouchi, *J. Chem. Phys.*, **17**, 245 (1949).
8. C. G. Opaskar, Ph. D. Thesis, University of Michigan, Ann Arbor, Michigan, 1966.